

Unpolarized structure functions and the parton distributions for nucleon in an independent quark model

N BARIK and R N MISHRA*

Department of Physics, Utkal University, VaniVihar, Bhubaneswar 751 004, India

*Department of Physics, Dhenkanal College, Dhenkanal 759 001, India

MS received 6 June 2000; revised 6 October 2000

Abstract. Considering the nucleon as consisting entirely of its valence quarks confined independently in a scalar-vector harmonic potential; unpolarized structure functions $F_1(x, \mu^2)$ and $F_2(x, \mu^2)$ are derived in the Bjorken limit under certain simplifying assumptions; from which valence quark distribution functions $u_v(x, \mu^2)$ and $d_v(x, \mu^2)$ are appropriately extracted satisfying the normalization constraints. QCD-evolution of these input distributions from a model scale of $\mu^2 = 0.07 \text{ GeV}^2$ to a higher Q^2 scale of $Q_0^2 = 15 \text{ GeV}^2$ yields $xu_v(x, Q_0^2)$ and $xd_v(x, Q_0^2)$ in good agreement with experimental data. The gluon and sea-quark distributions such as $G(x, Q_0^2)$ and $q_s(x, Q_0^2)$ are dynamically generated with a reasonable qualitative agreement with the available data; using the leading order renormalization group equations with appropriate valence-quark distributions as the input.

Keywords. Scalar-vector harmonic potential model; structure functions; parton distributions; momentum sum rule.

PACS Nos 13.60.Hb; 12.39.pn

1. Introduction

In QCD quark-parton model at the leading order; deep-inelastic lepton nucleon scattering is described in terms of the unpolarized nucleon structure functions $F_1(x, Q^2)$ and $F_2(x, Q^2)$ which are expressed as the charge squared weighted combinations of quark-parton distribution functions in Bjorken variable x . These distribution functions play an important role in the standard model phenomenology providing a deeper understanding of the quark gluon structure of the nucleon at very high energy. Therefore many experiments have been made to measure the deep-inelastic structure functions from which parton distributions inside the nucleon at very high energy have been extracted [1,2]. However for a complete knowledge and understanding of these distributions; some theoretically reasonable models are essential. Although perturbative QCD successfully relates the structure functions at different Q^2 [3]; it has not been possible to obtain the required input distribution function at a lower reference scale $Q^2 = \mu^2$ from a first principle calculation, because

of the inadequate understanding of the non-perturbative QCD in the confinement domain. Lattice QCD, as the favourite first principle technique has been pursued recently in this context [4]. Nevertheless it does involve inevitably increasing computational complexity in arriving at any desirable precision in its prediction. Therefore the input distribution functions at a lower reference scale, required in the Q^2 -evolution process to obtain the parton distributions at experimentally relevant higher Q^2 -values, are usually taken in suitable parametrized forms, which are fitted ultimately after the evolution with the available experimental data. There has also been attempts to derive the distribution functions at the bound state scales of the nucleons described by the low energy QCD-inspired phenomenological models. Such an approach can as well provide an interesting link between the low energy constituent quark models with the high energy parton picture of the hadrons; which may provide better understanding of the parton distribution in nucleons inside the nucleus and also the quark contribution to the proton spin.

Following the pioneering work of Jaffe [5] based on the MIT-Bag model; there has been several attempts [6–13] for the theoretical evaluation of deep-inelastic structure functions. The structure functions obtained in these models at a very low resolution scale, corresponding to the bound state scale of $Q^2 = \mu^2 \simeq \mathcal{O}(\Lambda_{\text{QCD}}^2)$, is considered to represent the leading twist non-singlet part of the physical structure function. Therefore one needs to evolve them appropriately through QCD-evolution equations [3] to the experimentally relevant higher Q^2 region for a comparison with the available data. All these calculations however yield more or less reasonable results mostly by way of fitting the experimental data with the Q^2 -evolved structure functions or the valence quark distributions realized from the model input expressions. Nevertheless, in most of these calculations the problem of fixing the model parameters remains.

We would intend here to derive the explicit functional forms for the unpolarized nucleon structure functions in an alternative constituent quark model of independent quarks confined by an effective scalar-vector harmonic potential in a Dirac formalism; whose model parameters had already been fixed earlier at the level of hadron spectroscopy and static hadron properties [14,15]. Our purpose here would be to investigate to what extent the input structure functions obtained at the model scale when evolved to high Q^2 yield results comparable with the experimental data at least at a qualitative level without insisting on quantitative precision. The predictive power of the model to be adopted here has been amply demonstrated in wide ranging low energy hadronic phenomena which include the weak and electromagnetic decays of light and heavy flavor mesons [16], elastic form factors and charge radii of nucleon [14], pion and K -meson [16] and the electromagnetic polarizability of proton [18]. Recently this model has also been successfully used in the study of the deep-inelastic polarized structure functions $g_1^P(x, Q^2)$ and $g_2^P(x, Q^2)$ of the proton [19]. Therefore we expect that by extending this model to the study of the unpolarized structure functions of the nucleon; it would provide a useful link between this low-energy constituent quark model and its corresponding high energy parton description of the nucleon.

In adopting this model here; we take the approximation of no gluon and sea-quark contents for the nucleon at some static point $Q^2 = \mu^2$ to consider the deep-inelastic scattering of electrons off the valence quarks only. The model solutions for the bound valence quark eigenmodes provide the essential model input in expressing the electromagnetic currents which ultimately define the relevant hadronic tensor for the deep-inelastic process. Explicit functional forms of the unpolarized structure functions are then derived analytically from the symmetric part of the hadronic tensor in the Bjorken limit with certain simpli-

fying assumptions; which on appropriate comparison with the parton model interpretation yields the valence quark distributions at the model scale of a low $Q^2 = \mu^2 \simeq \mathcal{O}(\Lambda_{\text{QCD}}^2)$. The support problem encountered in the present derivation is found to be rather minimal with structure functions falling off very rapidly to zero beyond $x = 1$. In spite of this apparent inadequate behaviour at and beyond the kinematic boundary; the overall suitability of the valence distribution functions obtained here can be tested through the normalization constraints; which are in fact found to be satisfied approximately within the limits of the kinematic boundaries. However if we extend the upper limit of the normalization integral from $x = 1$ to ∞ ; analytic evaluation of the integral yields the exact normalizations, demonstrating the minimal effects of the support problem. Therefore we believe that the valence distributions so extracted at the bound state scale can provide adequate model based inputs for appropriate QCD-evolution to experimentally relevant high Q^2 region for a qualitative comparison with the experimental data.

The paper is organized in the following manner. In §2, we discuss briefly the basic formalism with the necessary kinematics and derive the unpolarized structure functions $F_1(x, Q^2)$ and $F_2(x, Q^2)$ for the nucleon in the present model from the symmetric part of the hadronic tensor under certain simplifying assumptions in the Bjorken limit. Section 3 provides an appropriate parton model interpretation of the structure function $F_1(x, Q^2)$ which enables us to extract the valence quark distribution functions $u_v(x, Q^2)$ and $d_v(x, Q^2)$ at the model scale of low $Q^2 = \mu^2$ (which is not evident in these closed form expressions) as explicit functions of Bjorken variable x only. The valence distributions are found to saturate the required normalization constraints quite satisfactorily. The bound state scale of low $Q^2 = \mu^2$ is fixed on the basis of the renormalization group equations [13] by taking the experimental data of the momentum carried by the valence quarks at $Q_0^2 = 15 \text{ GeV}^2$ and also at the model scale $Q^2 = \mu^2$. Then the valence distribution function $u_v(x, Q^2) = 2d_v(x, Q^2)$ is evolved to the reference scale $Q_0^2 = 15 \text{ GeV}^2$ using the QCD-nonsinglet evolution equation, which are then utilized to evaluate the valence parts of the structure functions such as $[F_2^P(x, Q_0^2)]_v$, $[F_2^n(x, Q_0^2)]_v$ and that of the combination $[F_2^P(x, Q_0^2) - F_2^n(x, Q_0^2)]_v = \frac{x}{3}[u_v(x, Q_0^2) - d_v(x, Q_0^2)]$ for a comparison with the available experimental data. In §4, we attempt to obtain the gluon and the sea quark distribution in the form of $G(x, Q_0^2)$ and $q_s(x, Q_0^2)$ respectively; which are dynamically generated via well-known leading order renormalization group equations [20,21], with the valence distributions as the inputs. Then before attempting any specific flavor decomposition of the quark sea; we evaluate the momentum fraction carried by the quark-sea; the gluons as well as the valence quarks at $Q_0^2 = 15 \text{ GeV}^2$; which saturate the momentum sum rule. Finally to realize the complete structure functions $F_2^{(p,n)}(x, Q_0^2)$ and their difference $[F_2^P(x, Q_0^2) - F_2^n(x, Q_0^2)]$ which takes into account appropriate sea contributions together with their valence parts; we consider some specific prescription for the flavor decomposition of the sea. The structure functions so calculated are then compared with the available experimental data. Section 5 provides a brief summary and conclusion.

2. Structure functions in the model

The deep-inelastic electron-nucleon scattering is usually described by the hadronic tensor which is expressed as the Fourier transform of single nucleon matrix element of the commutator of two electromagnetic currents such as

$$W_{\mu\nu} = \frac{1}{4\pi} \int d^4\xi e^{iq\xi} \langle P, S | [J_\mu(\xi), J_\nu(0)] | P, S \rangle, \quad (2.1)$$

where q is the virtual photon four-momentum and P and S are the four-momentum and spin of the target nucleon respectively such that $P^\mu P_\mu = M^2$, $S^\mu S_\mu = -M^2$ and $P^\mu S_\mu = 0$. The conventional kinematic variables are defined usually as $Q^2 = -q^2 > 0$ and $x = Q^2/2\nu$; when $\nu = P \cdot q$ and $0 \leq x \leq 1$. In the rest frame of the target nucleon; one takes $P \equiv (M, 0, 0, 0)$ and $q \equiv (\nu/M, 0, 0, \sqrt{\nu^2/M^2 + Q^2})$. The nucleon state $|P, S\rangle$ in eq. (2.1) is normalized as $\langle P, S | P', S' \rangle = (2\pi)^3 2E \delta^3(\mathbf{P} - \mathbf{P}') \delta_{SS'}$. $W_{\mu\nu}$ in eq. (2.1) can be decomposed into a symmetric part $W_{\mu\nu}^{(S)}$ and an antisymmetric part $W_{\mu\nu}^{(A)}$ respectively; when it is the symmetric part $W_{\mu\nu}^{(S)}$ that defines the spin averaged structure functions F_1 and F_2 . The covariant expansion of $W_{\mu\nu}^{(S)}$ in terms of the scalar functions $W_1(x, Q^2)$ and $W_2(x, Q^2)$ provides its model independent description as

$$W_{\mu\nu}^{(S)} = \left[-g_{\mu\nu} + \frac{q_\mu q_\nu}{q^2} \right] W_1(x, Q^2) + \left[\left(P_\mu - q_\mu \frac{P \cdot q}{q^2} \right) \left(P_\nu - q_\nu \frac{P \cdot q}{q^2} \right) \right] \frac{W_2(x, Q^2)}{M^2}. \quad (2.2)$$

The unpolarized structure functions $F_1(x, Q^2)$ and $F_2(x, Q^2)$ which become the scaling functions of the Bjorken variable x in the Bjorken limit ($Q^2 \rightarrow \infty$, $\nu \rightarrow \infty$ with x fixed) are defined as $F_1(x, Q^2) \equiv W_1(x, Q^2)$ and $F_2(x, Q^2) \equiv \nu W_2(x, Q^2)/M^2$. It is well-known that while the structure function $F_1(x, Q^2)$ provides the contributions of the transverse virtual photons; a combination such as $W_L(x, Q^2) = [F_2(x, Q^2)/2x - F_1(x, Q^2)]$ owes it to the longitudinal virtual photons. It can be shown that $W_L(x, Q^2) = \frac{2M^2 x}{\nu} W_{00}^{(S)}$; so that with $W_{00}^{(S)}$ as finite in the Bjorken limit; $W_L \rightarrow 0$ satisfying thus the so called Callen Gross relation [22]

$$F_2(x, Q^2) = 2xF_1(x, Q^2). \quad (2.3)$$

Therefore for a model derivation of the structure functions one can start with eq. (2.1) with a static no gluon approximation for the target nucleon considered at rest. The nucleon state $|P, S\rangle$ in eq. (2.1) can be expressed in terms of its normalized SU(6)-spin flavor configuration denoted by $|N, S\rangle$ so that;

$$|P, S\rangle = [(2\pi)^3 2M \delta^3(0)]^{1/2} |N, S\rangle. \quad (2.4)$$

Then eq. (2.1) can be recast into a more suitable form [5] as;

$$W_{\mu\nu}(q, S) = \frac{M}{2\pi} \int_{-\infty}^{+\infty} dt e^{iq_0 t} \int d^3\mathbf{r}_1 \int d^3\mathbf{r}_2 e^{-iq \cdot (\mathbf{r}_1 - \mathbf{r}_2)} \times \langle N, S | [J_\mu(\mathbf{r}_1, t), J_\nu(\mathbf{r}_2, 0)] | N, S \rangle. \quad (2.5)$$

The electromagnetic current of the target nucleon is taken here in the form $J_\mu(\xi) = \sum_q e_q \bar{\psi}_q(\xi) \gamma_\mu \psi_q(\xi)$; where e_q is the electric charge of the valence quark of flavor q inside the nucleon. Expansion of the current commutator in $W_{\mu\nu}(q, s)$ in a constituent quark model generates bound quark propagator in the expression. But the calculation of the

bound quark propagator in the model would be extremely complicated leading to the evaluation of the structure function prohibitively more difficult. This however differs from the usual free field Dirac propagator mainly by virtue of the confining interaction. If the confining interaction is believed to be negligible in the Bjorken limit and the constituent quark mass m_q is taken in the current mass limit; it can be possible to replace the bound quark propagator by the free quark propagator in the zero mass limit as

$$\lim_{m_q \rightarrow 0} S_D(x) = \frac{1}{(2\pi)^3} \int d^4 k k \epsilon(k_0) \delta(k^2) e^{\pm i k x}, \quad (2.6)$$

with $\epsilon(k_0) = \text{sign}(k_0)$; which can yield a meaningful calculation of the structure function in the model. Justification of such an argument has been demonstrated in one dimensional Bag model [5] by showing that the propagator in the Bjorken limit is independent of the confining boundary. Therefore without explicit verification that it gives the same result as the bound state propagator in the Bjorken limit; free space propagator has also been used in three dimensional Bag model calculation of the nucleon structure function. We have adopted the same approximation in our earlier work on the calculation of spin dependent structure function in the present model [19]; where the quark mass parameter has been taken in the current mass limit as $m_q = 10$ MeV. Thus with the quark propagator taken as in eq. (2.6); the symmetric part of the hadronic tensor $W_{\mu\nu}^{(S)}$ can be obtained as

$$W_{\mu\nu}^{(S)} = [g_{\mu\lambda} g_{\nu\sigma} + g_{\mu\sigma} g_{\nu\lambda} - g_{\mu\nu} g_{\lambda\sigma}] T^{\lambda\sigma}. \quad (2.7)$$

Here

$$T^{\lambda\sigma} = \frac{M}{(2\pi)^4} \sum_q e_q^2 \int d^4 k k^\lambda \epsilon(k_0) \delta(k^2) \int_{-\infty}^{+\infty} dt e^{i(q_0+k_0)t} \\ \times \int d^3 \mathbf{r}_1 d^3 \mathbf{r}_2 e^{-i(\mathbf{q}+\mathbf{k}) \cdot (\mathbf{r}_1 - \mathbf{r}_2)} \langle \Gamma^\sigma \rangle, \quad (2.8)$$

and

$$\langle \Gamma^\sigma \rangle = \langle N, S | [\bar{\psi}_q(\mathbf{r}_1, t) \gamma^\sigma \psi_q(\mathbf{r}_2, 0) - \bar{\psi}_q(\mathbf{r}_2, 0) \gamma^\sigma \psi_q(\mathbf{r}_1, t)] | N, S \rangle. \quad (2.9)$$

Since it is evident from eq. (2.2) that $F_1(x, Q^2) = W_1(x, Q^2)$ is the coefficient of $(-g_{\mu\nu})$ in the covariant expansion of $W_{\mu\nu}^{(S)}$; eq. (2.7) in the same token can yield

$$F_1(x, Q^2) = g_{\lambda\sigma} T^{\lambda\sigma} \quad (2.10)$$

from which $F_2(x, Q^2)$ would follow through the Callen Gross relation. This provides the basic framework necessary for the derivation of structure function in a constituent quark model.

In the present model we express the quark field operators $\psi_q(\mathbf{r}, t)$ and hence $\bar{\psi}_q(\mathbf{r}, t)$ by their possible expansion in terms of the bound quark/anti-quark eigenmodes derivable in model as

$$\psi_q(\mathbf{r}, t) = \sum_\zeta [b_{q\zeta} \Phi_{q\zeta}^{(+)}(\mathbf{r}) e^{-i\mathbf{E}_{q\zeta} t} + \tilde{\mathbf{b}}_{q\zeta}^\dagger \Phi_{q\zeta}^{(-)}(\mathbf{r}) e^{i\mathbf{E}_{q\zeta} t}], \quad (2.11)$$

where $\tilde{b}_{q\zeta}^\dagger$ is the antiquark creation operator and $b_{q\zeta}$ is the quark annihilation operator corresponding to flavor q in the eigenmodes represented by the set of all the Dirac quantum numbers $\zeta \equiv (n, k, j)$. $\Phi_{q\zeta}^{(\pm)}(\mathbf{r})$ are the possible eigenmodes with respective eigenvalues as $E_{q\zeta}$ which provide in principle the basis set for the expansion in eq. (2.11). In the actual calculation of the relevant expectation value $\langle \Gamma^\sigma \rangle$ in eq. (2.9) with respect to the nucleon ground state; only the ground state positive energy eigenmodes $\Phi_{q\zeta_0}^{(+)}(\mathbf{r})$ would effectively contribute. In the present model with the independent quark confining potential $V(r) = (1/2)(1 + \gamma^0)(ar^2 + V_0)$, they are realized as [14]

$$\Phi_{q\zeta_0}^{(+)}(\mathbf{r}) = \frac{1}{\sqrt{4\pi}} \left(\begin{array}{c} ig_q(r)/r \\ \vec{\sigma} \cdot \hat{\mathbf{r}} f_q(r)/r \end{array} \right) \chi_{\zeta_0}, \quad (2.12)$$

where

$$\begin{aligned} g_q(r) &= N_q (r/r_{0q}) e^{-r^2/2r_{0q}^2}, \\ f_q(r) &= -\frac{N_q}{\lambda_q r_{0q}} (r/r_{0q})^2 e^{-(r^2/2r_{0q}^2)}. \end{aligned} \quad (2.13)$$

With $E'_q = (E_{q\zeta_0} - V_0/2)$, $m'_q = (m_q + V_0/2)$, $\lambda_q = (E'_q + m'_q)$ and $r_{0q} = (a\lambda_q)^{-1/4}$; the normalization factor N_q is given by

$$N_q^2 = \frac{8\lambda_q}{\sqrt{\pi}r_{0q}} \frac{1}{(3E'_q + m'_q)} \quad (2.14)$$

and the valence quark binding energy $E_q = E_{q\zeta_0}$ in the ground state is derivable from the bound state condition

$$(\lambda_q/a)^{1/2}(E'_q - m'_q) = 3. \quad (2.15)$$

χ_{ζ_0} in eq. (2.12) represents the spin up and spin down Pauli spinors $\chi_\uparrow = \begin{pmatrix} 1 \\ 0 \end{pmatrix}$ and $\chi_\downarrow = \begin{pmatrix} 0 \\ 1 \end{pmatrix}$ respectively. All these provide a brief outline of the essential elements of the model necessary for the derivation of the structure functions from eq. (2.10).

Now substituting eq. (2.11) in eq. (2.9) and keeping only the relevant contributing terms in $\langle \Gamma^\sigma \rangle$, eq. (2.10) with eq. (2.8) can be expressed as

$$F_1(x, Q^2) = [f_+(x, Q^2) - f_-(x, Q^2)], \quad (2.16)$$

where with $\langle \hat{n}_{q,\zeta_0} \rangle = \langle NS | \hat{b}_{q,\zeta_0}^\dagger \hat{b}_{q,\zeta_0} | NS \rangle$ and $\mathbf{K} = (\mathbf{q} + \mathbf{k})$;

$$\begin{aligned} f_+(x, Q^2) &= \frac{M}{(2\pi)^3} \sum_{q,\zeta_0} e_q^2 \langle \hat{n}_{q,\zeta_0} \rangle \int d^4k \epsilon(k_0) \delta(k^2) \int d^3\mathbf{r}_1 d^3\mathbf{r}_2 e^{-i\mathbf{K} \cdot (\mathbf{r}_1 - \mathbf{r}_2)} \\ &\quad \times [\bar{\Phi}_{q\zeta_0}^{(+)}(\mathbf{r}_1) \not{\mathbf{k}} \Phi_{q\zeta_0}^{(+)}(\mathbf{r}_2)] \delta(k_0 + q_0 + E_q), \end{aligned} \quad (2.17)$$

and

Parton distributions

$$\begin{aligned}
 f_-(x, Q^2) &= \frac{M}{(2\pi)^3} \sum_{q, \zeta_0} e_q^2 \langle \hat{n}_{q, \zeta_0} \rangle \int d^4 k \epsilon(k_0) \delta(k^2) \\
 &\quad \times \int d^3 \mathbf{r}_1 d^3 \mathbf{r}_2 e^{-i\mathbf{K} \cdot (\mathbf{r}_1 - \mathbf{r}_2)} \\
 &\quad \times \left[\bar{\Phi}_{q\zeta_0}^{(+)}(\mathbf{r}_2) \not{k} \Phi_{q\zeta_0}^{(+)}(\mathbf{r}_1) \right] \delta(k_0 + q_0 - E_q). \tag{2.18}
 \end{aligned}$$

Here the struck quark momentum \mathbf{K} is such that $|\mathbf{K}| = K \geq \bar{K} = (|\mathbf{q}| - |\mathbf{k}|)$; which can be reasonably assumed to be much less than q_0 , $|\mathbf{q}|$ and $|\mathbf{k}|$ in the Bjorken limit. The delta function appearing in eqs (2.17) and (2.18) implies the respective value of $|\mathbf{k}| = k$ as $k_+ = (q_0 + E_q)$ and $k_- = (q_0 - E_q)$ with $k_0 = -(q_0 + E_q)$ and $-(q_0 - E_q)$ respectively which are always negative in the Bjorken limit. This would lead to certain kinematic relations relevant in further simplifying the expressions $f_{\pm}(x, Q^2)$ in the Bjorken limit, which are as follows;

$$\begin{aligned}
 \bar{K} &\equiv \bar{K}_{\pm}(x) = |(E_q \mp Mx)|, \\
 \cos \theta_K &\simeq (Mx \mp E_q)/K, \\
 \cos \theta_K \cos \theta_k &\simeq -(Mx \mp E_q)/K, \\
 d(\cos \theta_k) k_{\pm}^2 &\simeq K dK. \tag{2.19}
 \end{aligned}$$

It may further be noted that with SU(2)-flavor symmetry the terms in the square brackets in eqs (2.17) and (2.18); would be independent of flavor and spin quantum numbers so as to be decoupled from the spin flavor summation. Therefore one can independently evaluate $\sum_{q, \zeta_0} \langle \hat{n}_{q, \zeta_0} \rangle e_q^2$ for the spin up proton target as 1 and the same for the neutron target as 2/3. This would apparently lead to the fact that the structure function $F_2^n(x, Q^2)$ would be in a constant ratio 2/3 with $F_2^P(x, Q^2)$ at the model scale of low Q^2 with only the valence quarks in the nucleon. Now further simplification of eqs (2.17) and (2.18) as per the discussions above in the case of the proton target yields

$$\begin{aligned}
 f_{\pm}^P(x, Q^2) &= \frac{M}{2\pi} \int_{\bar{K}_{\pm}}^{\infty} dK K [l_0^2(K) + l_1^2(K) \\
 &\quad + \frac{2}{K} (E_q - Mx) l_0(K) l_1(K)]; \tag{2.20}
 \end{aligned}$$

where

$$\begin{aligned}
 l_0(K) &= \int_0^{\infty} dr r g_q(r) j_0(Kr) \\
 &= \left(\frac{\pi}{2}\right)^{1/2} N_q r_{0q}^2 e^{-r_{0q}^2 K^2/2}, \\
 l_1(K) &= \int_0^{\infty} dr r f_q(r) j_1(Kr) \\
 &= -\left(\frac{\pi}{2}\right)^{1/2} \left(\frac{N_q}{\lambda_q}\right) r_{0q}^2 K e^{-r_{0q}^2 K^2/2}. \tag{2.21}
 \end{aligned}$$

Then the explicit functional form of the unpolarized structure function $F_1^P(x, Q^2)$ for the proton can be obtained in the present model through eq. (2.16) in terms of $f_{\pm}^P(x, Q^2)$ which can be evaluated in closed form from eq. (2.20) as

$$f_{\pm}^P(x, Q^2) = \frac{M N_q^2 r_{0q}^2}{8} \left[1 + \frac{K_{\pm}^2(x)}{\lambda_q^2} - \frac{2K_{\pm}(x)}{\lambda_q} + \frac{1}{\lambda_q^2 r_{0q}^2} \right] e^{-r_{0q}^2 K_{\pm}^2(x)}, \quad (2.22)$$

where $K_{\pm}(x) = (E_q \mp Mx)$. One can similarly find $F_1^n(x, Q^2)$ for the neutron; when $F_2^P(x, Q^2)$ and $F_2^n(x, Q^2)$ would follow using the Callen-Gross relation [22].

It may be noted here that $f_+^P(-x) = f_-^P(x)$ so that $F_1^P(-x) = -F_1^P(x)$ and $F_1^P(x)$ vanishes as $x \rightarrow 0$; being analytic there. Although Bjorken scaling is manifested here in the derived expression; the absence of the Regge-behaviour as well as the failure of $F_1^P(x)$ to vanish for $x > 1$ are the expected inadequacies near the kinematic boundaries which are the common pathological problems of all such constituent quark models. One can however take care of such inadequacies by making further refinements with translational and Lorentz invariance, which we propose to take up in our subsequent work. For a qualitative analysis we want to explore, how far is the model at this level able to predict the unpolarized structure functions and the parton distributions, without going into further complications. Thus for purely simplistic reasons one can proceed to extract the valence quark distributions $u_v(x, Q^2)$ and $d_v(x, Q^2)$ from $F_1^P(x)$ using its parton model interpretation appropriately.

3. Valence quark distribution functions

In the parton model picture at a low resolution scale; the nucleon can be considered to contain only (u, d) flavors for which quark parton distribution functions inside the nucleon can be defined in general as a combination of valence and sea components such as $u(x, Q^2) = u_v(x, Q^2) + u_s(x, Q^2)$ and $d(x, Q^2) = d_v(x, Q^2) + d_s(x, Q^2)$ with the corresponding antiparton distributions defined accordingly. Then as per the parton model descriptions

$$\begin{aligned} F_1^P(x, Q^2) &= 1/18[\{4u(x, Q^2) + d(x, Q^2)\} + \{4\bar{u}(x, Q^2) + \bar{d}(x, Q^2)\}], \\ F_1^n(x, Q^2) &= 1/18[\{4d(x, Q^2) + u(x, Q^2)\} + \{4\bar{d}(x, Q^2) + \bar{u}(x, Q^2)\}]. \end{aligned} \quad (3.1)$$

Now comparing expressions in eq. (3.1) with eq. (2.16) and attributing as usual in such model the negative part of the distribution in eq. (2.16) to the anti-partons in eq. (3.1); effective parton and antiparton distributions can be identified [5] as

$$\begin{aligned} u(x, Q^2) &= 2d(x, Q^2) = 4f_+^P(x, Q^2), \\ \bar{u}(x, Q^2) &= 2\bar{d}(x, Q^2) = -4f_-^P(x, Q^2). \end{aligned} \quad (3.2)$$

One may note here that the negative antiparton distribution so obtained at the model scale calculation, which turns out on explicit evaluation to be quantitatively negligible; can be treated only as a model artifact which in fact is encountered in all such constituent quark

models [5]. This spurious contribution needs to be appropriately eliminated in extracting the valence quark distribution correctly from the effective parton distributions in eq. (3.2). Thus keeping in mind that $\bar{u}_v(x, Q^2) = 0 = \bar{d}_v(x, Q^2)$ as per our initial assumption and considering the resulting spurious parton and antiparton sea to be symmetric (i.e. $u_s(x) = \bar{u}_s(x) = \bar{u}(x)$ and $d_s(x) = \bar{d}_s(x) = \bar{d}(x)$ etc); we get the appropriate valence distributions

$$u_v(x, Q^2) = 2d_v(x, Q^2) = 4[f_+^P(x, Q^2) + f_-(x, Q^2)]. \quad (3.3)$$

Thus the valence quark distribution functions $u_v(x, Q^2)$ and $d_v(x, Q^2)$ can be extracted at a model scale of low $Q^2 = \mu^2$ in terms of analytically obtained closed form expressions $f_{\pm}^P(x, Q^2)$ as explicit functions of the Bjorken variable x ; which can be evaluated by taking the model parameters and other relevant model quantities from some of its earlier applications [14,16,19] as

$$\begin{aligned} (a, V_0) &= (0.017166 \text{ GeV}^3, -0.1375 \text{ GeV}), \\ (m_u, m_d) &= (0.01 \text{ GeV}, 0.01 \text{ GeV}), \\ (E_q, \lambda_q) &= (0.45129 \text{ GeV}, 0.46129 \text{ GeV}), \\ (N_q, r_{0q}) &= (0.64318 \text{ GeV}^{1/2}, 3.35227 \text{ GeV}^{-1}). \end{aligned} \quad (3.4)$$

We may point out here that the physical mass M of the nucleon in this model can be realized only after taking into account other possible residual effects including the center of mass correction [14] in a perturbative manner which provide the corrected E_q so as to realize $M = 3E_q$. We therefore prefer here to take $E_q = M/3$ with $M = 0.9382 \text{ GeV}$. Numerical results for $xu_v(x, Q^2)$ and $xd_v(x, Q^2)$ as functions of x are shown in figures 1 and 2 respectively. Although the support problem is evidently present here, the extent of this inadequacy can be estimated through the normalization integral which comes out numerically as

$$\int_0^1 dx u_v(x, Q^2) = 1.988. \quad (3.5)$$

However if we extend the upper limit to $x = \infty$ and take into account the symmetry behaviour $u_v(-x) = u_v(x)$; we can analytically evaluate the integral to show that

$$\begin{aligned} \int_0^1 dx u_v(x, Q^2) &\equiv 1/2 \int_{-\infty}^{\infty} dx u_v(x, Q^2) \\ &= 4 \int_{-\infty}^{\infty} dx f_+^P(x, Q^2) \\ &= 1/2 \sqrt{\pi} N_q^2 r_{0q} \left(1 + \frac{3}{2\lambda_q^2 r_{0q}^2} \right) = 2. \end{aligned} \quad (3.6)$$

This shows that not only the support problem in the integrated sense is rather minimal; the valence distributions so extracted saturate the normalization constraint quite satisfactorily. Therefore we may be justified in using these valence distributions to realize further the valence parts of the structure functions such as $[F_2^P(x, Q^2)]_v = \frac{1}{2}xu_v(x, Q^2)$ and $[F_2^n(x, Q^2)]_v = \frac{1}{3}xu_v(x, Q^2)$ as well as the same for the combination $[F_2^p(x, Q^2) -$

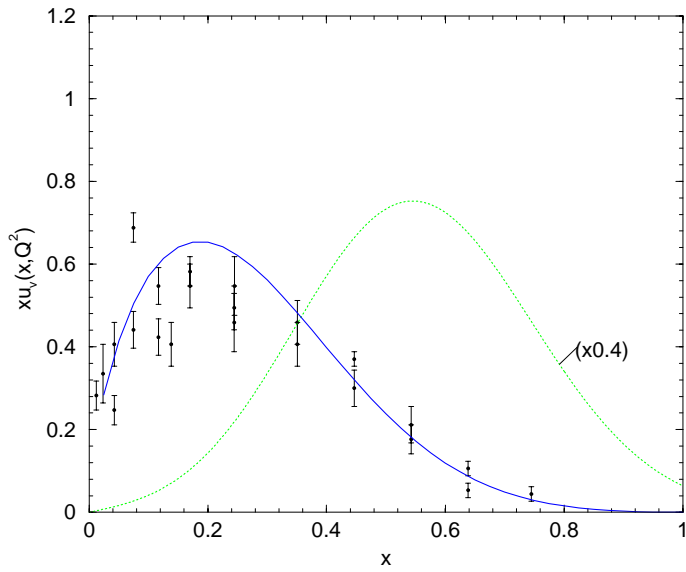


Figure 1. The calculated $xu_v(x, Q^2)$ at $Q^2 = \mu^2 = 0.07 \text{ GeV}^2$ (dotted line) and QCD evolved result at $Q_0^2 = 15 \text{ GeV}^2$ (solid line) compared with the data taken from T Sloan *et al* in ref. [2].

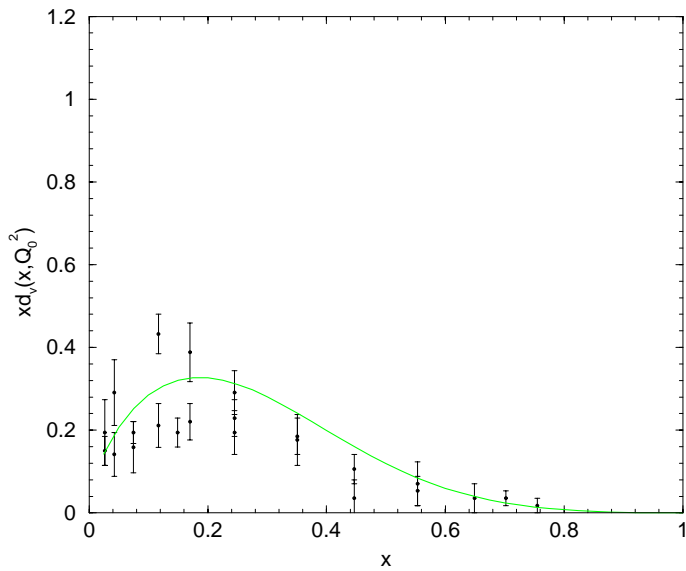


Figure 2. The QCD evolved result for $x d_v(x, Q^2)$ at $Q_0^2 = 15 \text{ GeV}^2$ (solid line) is given in comparison with the experimental data taken from T Sloan *et al* in ref. [2].

$F_2^n(x, Q^2)]_v \simeq \frac{1}{6} x u_v(x, Q^2)$; which can be numerically evaluated in the kinematic range of the Bjorken variable x . These results which correspond to a model scale of low $Q^2 = \mu^2$; are not directly comparable with the experimental data available at high Q^2 . Therefore one needs appropriate QCD-evolution of the valence distributions from the model scale to the experimentally relevant higher Q^2 .

The model scale of low $Q^2 = \mu^2$ is neither explicit in the derived expressions for the structure functions nor in the valence distributions $u_v(x, Q^2)$ and $d_v(x, Q^2)$. Therefore we need to first fix the model scale $Q^2 = \mu^2$. We obtain this with the help of the renormalization group equation [13], as per which

$$\mu^2 = \Lambda_{\text{QCD}}^2 e^L; \quad (3.7)$$

where $L = [V^{n=2}(Q_0^2)/V^{n=2}(\mu^2)]^{1/a_N^{n=2}} \ln(\frac{Q_0^2}{\Lambda_{\text{QCD}}^2})$ with $V^{n=2}(Q^2) = \int_0^1 dx x [u_v(x, Q^2) + d_v(x, Q^2)]$ as the momentum carried by the valence quarks at Q^2 . Now taking the experimental reference scale $Q_0^2 = 15 \text{ GeV}^2$ for which $V^{n=2}(15 \text{ GeV}^2) \simeq 0.4$ [2,8] with $\Lambda_{\text{QCD}} = 0.232 \text{ GeV}$ and $a_N^{n=2} = 32/81$ for 3-active flavors; we can obtain $\mu^2 \simeq 0.07 \text{ GeV}^2$. If one believes that the perturbation theory still makes sense down to this model scale for which the relevant perturbative expansion parameter $\alpha_s(\mu^2)/2\pi$ is less than one ($\simeq 0.85$ here), one can evolve the valence distributions $u_v(x, \mu^2) = 2d_v(x, \mu^2)$ to higher Q_0^2 , where experimental data are available. In fact one does not have much choice here, because taking any higher model scale on adhoc basis would require a non-zero initial input of sea quark and gluon constituents for which one does not have any dynamical information at such scale and hence it would complicate the picture. Therefore when $\alpha_s(\mu^2)/2\pi$ is well within the limit to justify the applicability of perturbative QCD at the leading order and further since non-singlet evolution is believed to converge very fast [23] to remain stable even for small values of $Q^2/\Lambda_{\text{QCD}}^2$; one may think of a reliable interpolation between the low model scale of $Q^2 = \mu^2 < 0.1 \text{ GeV}^2$ and the experimentally relevant higher $Q^2 \gg \mu^2$, if one does not insist upon quantitative precision. With such justification and belief many authors in the past have used the choice of low $Q^2 = \mu^2$ (for example; $\mu^2 = 0.063 \text{ GeV}^2$ [9], 0.068 GeV^2 , 0.09 GeV^2 [10] and 0.06 GeV^2 [12]) as their static point for evolution. In fact the choice of low $Q^2 = \mu^2 < 0.1 \text{ GeV}^2$ in such models is linked with the initial sea and gluon distributions taken approximately zero at the model scale. Following such arguments we choose to evolve the valence distributions by the standard convolution technique based on nonsinglet evolution equations in leading order [3,23] from the static point of $\mu^2 = 0.07 \text{ GeV}^2$ to $Q_0^2 = 15 \text{ GeV}^2$ for a comparison with the experimental data. Our results for $xu_v(x, Q_0^2)$ and $xd_v(x, Q_0^2)$ at $Q_0^2 = 15 \text{ GeV}^2$ are provided in figures 1 and 2 respectively along with the experimental data, which on comparison shows very satisfactory agreement over the entire range $0 \leq x \leq 1$. The valence components of the structure functions such as $[F_2^P(x, Q_0^2)]_v$ and $[F_2^n(x, Q_0^2)]_v$ together with the valence part of the combination $[F_2^P(x, Q_0^2) - F_2^n(x, Q_0^2)]$ calculated at $Q_0^2 = 15 \text{ GeV}^2$, are also compared with the respective experimental data in figures 3, 4 and 5 respectively. We find that the agreement with the data in all these cases is reasonably much better in the region $x > 0.2$. This is because in the small x region; the sea contributions to the structure functions not included in the calculation so far are significant enough to generate the appreciable departures from the data as observed here.

Therefore for a complete description of the nucleon structure functions and hence the parton distributions in the nucleon; the valence contributions discussed above need to be supplemented by the expected gluon and sea-quark contributions at high energies.

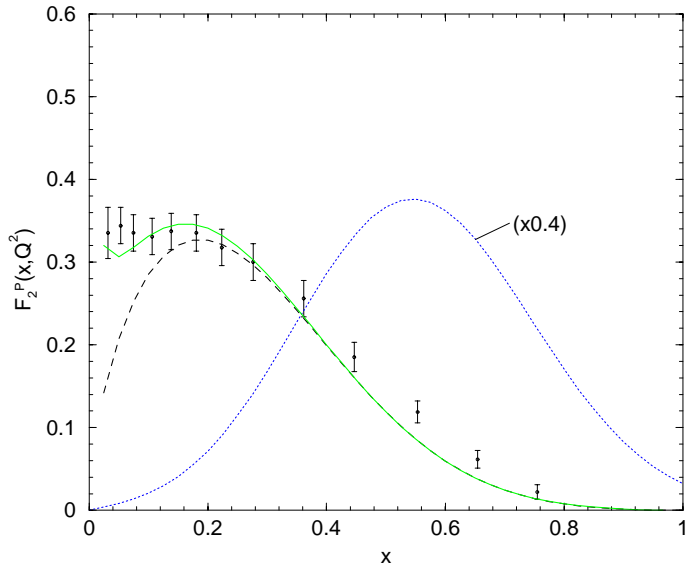


Figure 3. The calculated $[F_2^p(x, Q^2)]_{\text{val}}$ at $Q^2 = \mu^2 = 0.07 \text{ GeV}^2$ (dotted line) and QCD evolved result at $Q_0^2 = 15 \text{ GeV}^2$ (dashed line). $F_2^p(x, Q^2)$ (valence+asymmetric sea: solid line) in comparison with experimental data taken from Roberts *et al* in ref. [1].

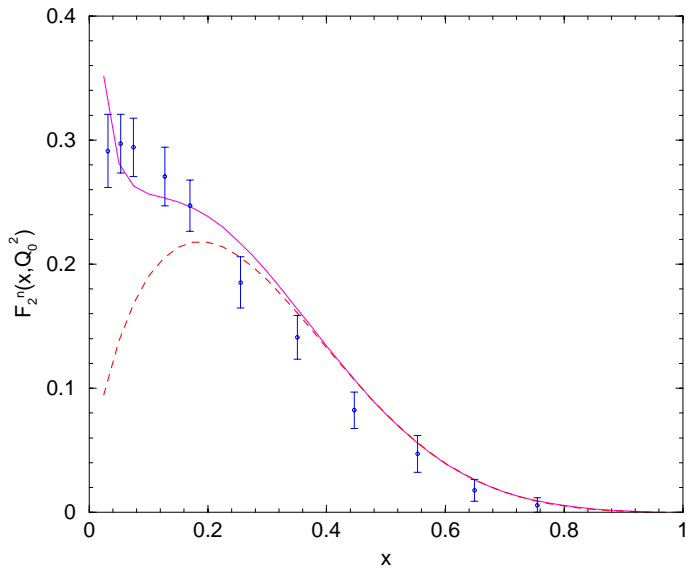


Figure 4. The QCD evolved result for $[F_2^n(x, Q^2)]_{\text{val}}$ at $Q_0^2 = 15 \text{ GeV}^2$ (dashed line) and $F_2^n(x, Q^2)$ (valence+asymmetric sea: solid line) in comparison with data from Roberts *et al* in ref. [1].

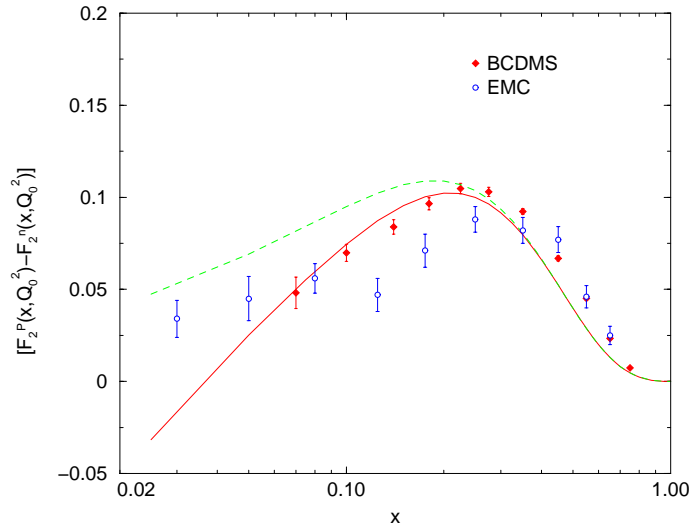


Figure 5. The QCD evolved result for $[F_2^P(x, Q_0^2) - F_2^N(x, Q_0^2)]$ (solid line; valence+asymmetric sea) at $Q_0^2 = 15 \text{ GeV}^2$ compared with the data. (Data is over the Q^2 -range of the experiments as per ref. [2].)

4. Gluon and sea-quark distributions

The gluon and the sea-quark distributions at high energy inside the nucleon can be generated purely radiatively with appropriate input of the valence distributions using the well-known leading order renormalization group (RG)-equations [23]. Considering that at higher energy, heavier flavors may be excited above each flavor threshold, we define the total sea quark distribution here up to three flavors as

$$q_s(x, Q^2) = 2[u_s(x, Q^2) + d_s(x, Q^2) + s_s(x, Q^2)] \quad (4.1)$$

and the gluon distribution by $G(x, Q^2)$. Their moments $q_s^n(Q^2)$ and $G^n(Q^2)$ respectively can be described in terms of the corresponding moment $V^n(Q^2)$ of the input valency distribution $V(x, Q^2) = [u_v(x, Q^2) + d_v(x, Q^2)]$ according to the RG-equations such as

$$G^n(Q^2) = \left[\frac{\alpha^n(1 - \alpha^n)}{\beta^n} L_0^{a_{N_s}^n} \{L_0^{-a_n^-} - L_0^{-a_n^+}\} \right] V^n(Q^2), \quad (4.2)$$

$$q_s^n(Q^2) = [L_0^{a_{N_s}^n} \{ \alpha^n L_0^{-a_n^-} + (1 - \alpha^n) L_0^{-a_n^+} - L_0^{-a_{N_s}^n} \}] V^n(Q^2), \quad (4.3)$$

where the n th moments of the functions $A(x, Q^2) \equiv \{G(x, Q^2), q_s(x, Q^2), V(x, Q^2)\}$ are defined as

$$A^n(Q^2) = \int_0^1 dx x^{n-1} A(x, Q^2), \quad (4.4)$$

and the RG-exponents such as $\{\alpha^n, \beta^n, a_{NS}^n, a_{\pm}^n\}$ in the conventional notations are derivable for the n th moment as per ref. [23]. Finally $L_0 = \frac{\alpha_s(\mu^2)}{\alpha_s(Q_0^2)} = \frac{\ln(Q_0^2/\Lambda_{\text{QCD}}^2)}{\ln(\mu^2/\Lambda_{\text{QCD}}^2)}$ is defined here in terms of the momentum carried by the valence quarks at Q_0^2 on the basis of the assumption of momentum saturation by valence quarks at the model scale $Q^2 = \mu^2$ as

$$L_0 = \left[\int_0^1 dx x V(x, Q_0^2) \right]^{-1/a_{NS}^{n=2}}; \tag{4.5}$$

when $a_{NS}^{n=2} = 32/81$ for three active flavors considered here. We may, however, point out here that although we have evolved the valence distributions from a model scale of 0.07 GeV^2 ; we find that due to the support problem, the net momentum carried by the valence quarks is saturated at $Q^2 \simeq 0.1 \text{ GeV}^2$ in our model but not at the model scale of 0.07 GeV^2 . Therefore for the input L_0 in eqs (4.2) and (4.3) we prefer to take $\mu^2 = 0.1 \text{ GeV}^2$ as the static point so that corresponding to the experimental reference scale $Q_0^2 = 15 \text{ GeV}^2$, $L_0 = \frac{\ln(Q_0^2/\Lambda_{\text{QCD}}^2)}{\ln(\mu^2/\Lambda_{\text{QCD}}^2)} \simeq 9.603$. Then calculating the appropriate RG-exponents as per ref. [23] for $n = 2, 4, 6, 8$ (higher moments being significantly smaller are not considered here) and the corresponding moments $V^n(Q_0^2 = 15 \text{ GeV}^2)$ from the evolved valence distribution $u_v(x, Q_0^2) = 2d_v(x, Q_0^2)$ at $Q_0^2 = 15 \text{ GeV}^2$; we evaluate the respective moments $G^n(Q_0^2)$ and $q_s^n(Q_0^2)$ from RG equations (4.2) and (4.3). Then the gluon and the sea-quark distributions can be extracted from the moments by the standard inverse Mellin-transform technique. However since we are not aiming at any quantitative precision here, we rather adopt a matrix inversion technique with the help of simple parametric expressions taken for $xG(x, Q_0^2)$ and $xq_s(x, Q_0^2)$ as

$$xG(x, Q_0^2) = [a_1 x^2 + a_2 x + a_3 + a_4/\sqrt{x}], \tag{4.6}$$

$$xq_s(x, Q_0^2) = [b_1 x^2 + b_2 x + b_3 + b_4/\sqrt{x}]. \tag{4.7}$$

The moments calculated from these parametric expressions would now provide a set of simultaneous equations for each set of parameters $\{a_i\}$ and $\{b_i\}$ separately. Solving these equations by matrix inversion method we arrive at the values of these parameters as

$$\begin{aligned} \{a_i, i = 1, 2, 3, 4\} &\equiv (-0.8473, 2.0144, -2.1059, 0.9314), \\ \{b_i, i = 1, 2, 3, 4\} &\equiv (-0.2208, 0.5103, -0.5108, 0.2193). \end{aligned} \tag{4.8}$$

Thus we generate somewhat reasonable functional forms for $xq_s(x, Q_0^2)$ and $xG(x, Q_0^2)$ at $Q_0^2 = 15 \text{ GeV}^2$ which are provided in figures 6 and 7 respectively in comparison with the available experimental data. We find the qualitative agreement with the data quite satisfactory with almost vanishing contribution in both cases beyond $x > 0.5$.

We find next the momentum distributions for different constituent partons at $Q_0^2 = 15 \text{ GeV}^2$ by calculating the second moments of the distribution functions $u_v(x, Q_0^2), d_v(x, Q_0^2), q_s(x, Q_0^2)$ and $G(x, Q_0^2)$ respectively so as to obtain them as

$$\begin{aligned} u_v(Q_0^2) &= 0.273, (0.275 \pm 0.011), \\ d_v(Q_0^2) &= 0.136, (0.116 \pm 0.017), \\ q_s(Q_0^2) &= 0.109, (0.074 \pm 0.011), \\ G(Q_0^2) &= 0.482, (0.535). \end{aligned} \tag{4.9}$$

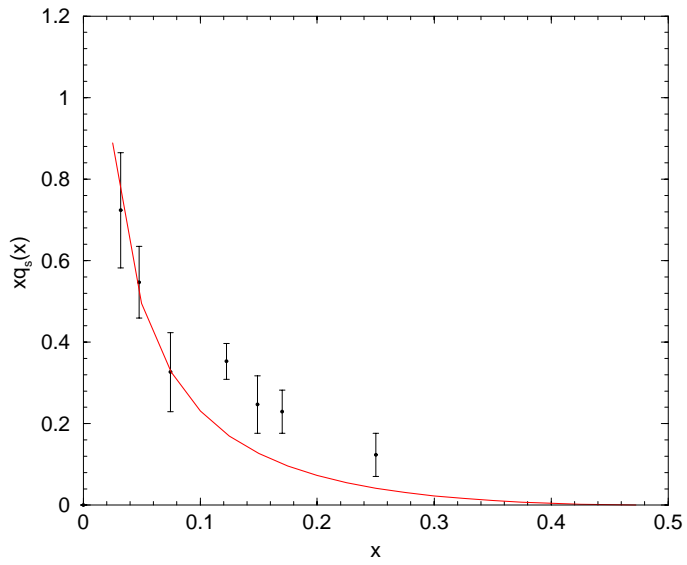


Figure 6. The dynamically generated $xq_s(x, Q^2)$ (solid line) at $Q_0^2 = 15 \text{ GeV}^2$, compared with the data from T Sloan *et al* in ref. [2].

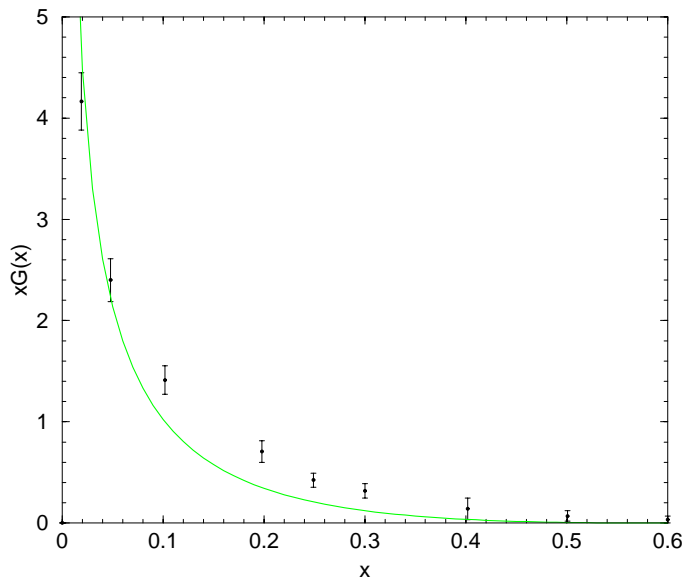


Figure 7. The dynamically generated $xG(x, Q^2)$ (solid line) at $Q_0^2 = 15 \text{ GeV}^2$, compared with the data from T Sloan *et al* in ref. [2].

The experimental values are shown within the brackets against the values calculated for a comparison. We find that the parton distributions realized at a qualitative level in the model at $Q_0^2 = 15 \text{ GeV}^2$ saturate the momentum sum-rule. Finally to evaluate the complete structure functions $F_2^{(p,n)}(x, Q_0^2)$ by supplementing the respective valence components with the necessary sea-contributions; we consider a flavor decomposition of the net sea-quark distribution $q_s(x, Q_0^2)$. With an old option of a complete symmetric sea in SU(3)-flavor sector;

$$[F_2^P(x, Q_0^2)]_{\text{sea}} = [F_2^n(x, Q_0^2)]_{\text{sea}} = \frac{2}{9} x q_s(x, Q_0^2). \quad (4.10)$$

However it has been almost established experimentally that the nucleon quark sea is flavor asymmetric both in SU(2) as well as SU(3) sector. Experimental violation of Gottfried sum rule [24] and more recent and precise asymmetry measurements in the Drell–Yan process with nucleon targets [25,26] have shown a strong x -dependence of the ratio $[d_s(x, Q^2)/u_s(x, Q^2)]$ with $d_s(x, Q^2) > u_s(x, Q^2)$ for $x < 0.2$ whereas $d_s(x, Q^2)$ running closer to $u_s(x, Q^2)$ for $x > 0.2$; when around $x = 0.18$; $d_s(x, Q^2) \simeq 2u_s(x, Q^2)$. Neutrino charm production experiment by CCFR collaboration [27] also provides evidence in favour of the relative abundance of strange to non-strange sea-quarks in the nucleon measured by a factor $\kappa \equiv \frac{2\langle x s_s \rangle}{\langle x u_s + x d_s \rangle} = 0.477 \pm 0.063$. Therefore keeping these experimental facts in mind we make a reasonable choice for the flavor structure of the sea quark distribution as defined in eq. (4.1) by taking

$$\begin{aligned} d_s(x, Q_0^2) &= 2u_s(x, Q_0^2), \\ s_s(x, Q_0^2) &= \frac{1}{4}[u_s(x, Q_0^2) + d_s(x, Q_0^2)]. \end{aligned} \quad (4.11)$$

Then we find the sea contributions to the structure functions $F_2^{(p,n)}(x, Q_0^2)$ as

$$\begin{aligned} [F_2^p(x, Q_0^2)]_{\text{sea}} &= \frac{1}{5} x q_s(x, Q_0^2), \\ [F_2^n(x, Q_0^2)]_{\text{sea}} &= \frac{13}{45} x q_s(x, Q_0^2). \end{aligned} \quad (4.12)$$

The results for the complete structure functions $F_2^p(x, Q_0^2)$ and $F_2^n(x, Q_0^2)$ with the valence and quark sea components taken together are shown in figures 3 and 4. We find that the overall qualitative agreement is quite reasonable for the region $x > 0.04$. But because of the theoretical as well as experimental uncertainties; one can not make a meaningful comparison of the data in the region $x < 0.1$. We have also shown in figure 5 the structure function combination $[F_2^p(x, Q_0^2) - F_2^n(x, Q_0^2)]$ by taking into account the asymmetric sea contribution as in eq. (4.12), which provides a relatively better agreement with the available experimental data over a Q^2 -range [2].

5. Summary and conclusion

Starting with a constituent quark model of relativistic independent quarks in an effective scalar-vector harmonic potential; we have been able to analytically derive an explicit

functional form for the deep-inelastic unpolarized nucleon structure function $F_1(x, Q^2)$ at the model scale of low $Q^2 = \mu^2 = 0.07 \text{ GeV}^2$ from which the valence quark distributions $u_v(x, Q^2)$ and $d_v(x, Q^2)$ have been appropriately extracted. The closed form expressions for $u_v(x, Q^2)$ and $d_v(x, Q^2)$ satisfying the normalization constraints provide suitable model inputs for QCD-evolution to experimentally relevant $Q^2 = Q_0^2 = 15 \text{ GeV}^2$. The valence distribution functions as $xu_v(x, Q_0^2)$ and $xd_v(x, Q_0^2)$; the valence components $[F_2^P(x, Q_0^2)]_v$ and $[F_2^n(x, Q_0^2)]_v$ as well as the valence part of the combination $[F_2^P(x, Q_0^2) - F_2^n(x, Q_0^2)]$ realized through QCD-evolution at $Q_0^2 = 15 \text{ GeV}^2$, compare reasonably well with the experimental data in the expected range of the Bjorken variable x .

The gluon distribution $G(x, Q_0^2)$ and the sea-quark distributions $q_s(x, Q_0^2)$ are dynamically generated from the renormalization group equations with the moments of valency quark distributions at $Q_0^2 = 15 \text{ GeV}^2$ as the inputs. The results for $xG(x, Q_0^2)$ and $xq_s(x, Q_0^2)$ make a good comparison with the data. Calculation of the constituent parton momenta also yields the momentum percentage in the valence-quark sector as 27.3% and 13.6% for the u and d -flavor quarks respectively, whereas it gives in the sea-quark sector 10.9% and in the gluon sector 48.2%; thereby saturating the expected momentum sum-rule. Incorporating the sea quark contributions to the valence part of the nucleon structure functions; the complete unpolarized structure functions $F_2^P(x, Q_0^2)$, $F_2^n(x, Q_0^2)$ and $[F_2^P(x, Q_0^2) - F_2^n(x, Q_0^2)]$ are obtained in reasonable agreement with the data in the region $x > 0.1$.

There are of course various finer features of the nucleon structure functions quite apart from their behaviour near the region $x = 0$; which would be beyond the limit of this simplistic approach in the model to address. Nevertheless within its limitations; the model is found to provide a simple parameter free analysis of the deep-inelastic unpolarized structure functions of the nucleon leading to the realization of its constituent parton distributions at $Q_0^2 = 15 \text{ GeV}^2$ with an over-all qualitative agreement with the experimental data. Proper corrections for the center of mass motion would be attempted in our future works.

Acknowledgements

We are thankful to Prof. B B Deo for many fruitful discussions and useful suggestions. We are also thankful to the Institute of Physics, Bhubaneswar, India for providing necessary library and computational facilities for doing this work. One of us (RNM) would like to express his gratitude to the Department of Higher Education, Government of Orissa; for providing study leave for this purpose.

References

- [1] R G Roberts and M R Whalley, *J. Phys.* **G17**, D1 (1991)
S R Mishra and F Sciulli, *Ann. Rev. Nucl. Part. Sci.* **39**, 259 (1989) and the references therein
J F Owens and W K Tung, *Ann. Rev. Nucl. Part. Sci.* **42**, 291 (1992)
A Milsztajn *et al*, *Z. Phys.* **C49**, 527 (1991) and the references therein
P Amaudruz *et al*, *Phys. Rev. Lett.* **66**, 2712 (1991)
- [2] T Sloan, G Smadja and R Voss, *Phys. Rep.* **162**, 45 (1988)
J J Aubert *et al*, *Nucl. Phys.* **B293**, 740 (1987)
New Muon Collaboration: D Allasia *et al*, Report No. CERN-PPE/90-103 (1990)

- BCDMS collaboration: A C Benvenuti *et al*, *Phys. Lett.* **B237**, 599 (1990)
- [3] G Altarelli and G Parisi, *Nucl. Phys.* **B126**, 298 (1977)
- [4] M Gökler *et al*, *J. Phys.* **G22**, 703 (1996)
- [5] R L Jaffe, *Phys. Rev.* **D11**, 1953 (1975)
- [6] C J Benesh and G A Miller, *Phys. Rev.* **D36**, 1344 (1987)
C J Benesh and G A Miller, *Phys. Rev.* **D38**, 48 (1988)
- [7] X M Wang, X Song and P C Yin, *Hadron J.* **6**, 985 (1983)
X M Wang, *Phys. Lett.* **B140**, 413 (1984)
- [8] X Song and J S Mc Carthy, *Phys. Rev.* **D49** 3169 (1994); **C46**, 1077 (1992)
- [9] H Meyer and P J Mulders, *Nucl. Phys.* **A528**, 589 (1991)
M Traini, L Conci and U Moschella, *Nucl. Phys.* **A544**, 731 (1992)
- [10] A W Schreiber, A I Signal and A W Thomas, *Phys. Rev.* **D44**, 2653 (1991)
M R Bate and A I Signal, *J. Phys.* **G18**, 1875 (1992)
- [11] T N Pham, *Phys. Rev.* **D19**, 707 (1979)
A Dhaul, A N Mitra and A Pagnamenta, *Z. Phys.* **C36**, 115 (1987)
M V Terentev, *Yad. Fiz. Sov. J. Nucl. Phys.* **24**, 207 (1976); 106 (1976)
Z Dziembowski, C J Martoff and P. Zyla, *Phys. Rev.* **D50**, 5613 (1994)
H J Weber, *Phys. Rev.* **D49**, 3160 (1994)
- [12] R P Bickerstaff and J L Londergan, *Phys. Rev.* **42**, 3621 (1990)
- [13] M Stratmann, *Z. Phys.* **C60**, 763 (1993)
- [14] N Barik, B K Dash and M Das, *Phys. Rev.* **D31**, 1652 (1985); **D32**, 1725 (1985)
N Barik and B K Dash, *Phys. Rev.* **D34**, 2092, 2803 (1986); **D33**, 1925 (1986)
- [15] N Barik, B K Dash and P C Dash, *Pramana – J. Phys.* **29**, 543 (1987)
- [16] N Barik, P C Dash and A R Panda, *Phys. Rev.* **D46**, 3856 (1992); **D47**, 1001 (1993)
N Barik and P C Dash, *Phys. Rev.* **D47**, 2788 (1993); **D53**, 1366 (1996)
N Barik, S Tripathy, S Kar and P C Dash, *Phys. Rev.* **D56**, 4238 (1997)
N Barik, S Kar and P C Dash, *Phys. Rev.* **D57**, 405 (1998)
- [17] N Barik *et al*, *Phys. Rev.* **D59**, 037301 (1999)
- [18] N Barik, B K Dash and A R Panda, *Nucl. Phys.* **A605**, 433 (1996)
- [19] N Barik and R N Mishra, *Phys. Rev.* **D61**, 014002 (2000)
- [20] G Parisi and R Petronzio, *Phys. Lett.* **B62**, 331 (1976)
V A Novikov, M A Shifman, A I Vainstein and V I Zakharov, *JETP Lett.* **24**, 341 (1976);
Ann.Phys. **105**, 276 (1977)
M Gluck and E Reya, *Nucl. Phys.* **B130**, 76 (1977)
- [21] M Gluck, R M Godbole and E Reya, *Z. Phys.* **C41**, 667 (1989)
- [22] Callen Gross relation is satisfied in the model here, since it can be shown that $W_{00}^{(S)}(x, Q^2)$ is finite in the Bjorken limit as $W_{00}^s = \frac{MN_q^2 r_{0q}^2}{8} \left[\left(1 + \frac{1}{\lambda_q^2 r_{0q}^2} + \frac{K_+^2}{\lambda_q^2} + \frac{2K_+}{\lambda_q} \right) e^{-r_{0q}^2 K_+^2} - (K_+ \rightarrow K_-) \right]$
- [23] M R Pennington and G G Ross, *Phys. Lett.* **B86**, 371 (1979)
A J Buras, *Rev. Mod. Phys.* **52**, 199 (1980)
Richard D Field, in *Application of perturbative-QCD* (Addison-Wesley, New York, 1989) p.148
- [24] M Arneodo *et al*, *Phys. Rev.* **D50**, R1 (1994)
P Amadruz *et al*, *Phys. Rev. Lett.* **66**, 2712 (1991)
- [25] NA51 Collaboration: A Baldit *et al*, *Phys. Lett.* **B332**, 244 (1994)
- [26] Fermilab E866/NuSea Collaboration: E A Hawker, *et al*, *Phys. Rev. Lett.* **80**, 3715 (1998)
- [27] CCFR Collaboration: A O Bazarko *et al*, *Z. Phys.* **C65**, 189 (1995)